Alkylidene Fluorene Liquid Crystalline Semiconducting Polymers for Organic Field Effect Transistor Devices

Martin Heeney, Clare Bailey, Mark Giles, Maxim Shkunov, David Sparrowe, Steve Tierney, Weimin Zhang, and Iain McCulloch*

Merck Chemicals, Chilworth Science Park, Southampton, SO16 7QD, UK

Received January 30, 2004; Revised Manuscript Received March 24, 2004

ABSTRACT: Organic electronic devices comprising arrays of organic field effect transistors (OFETs) are expected to create a range of novel applications for which the ability to be fabricated in large areas, on flexible substrates, with nonconventional shapes, and at low cost are key enabling factors. To improve the electrical performance of such devices, new solution processable organic semiconductors are required with high charge carrier mobilities and environmental stability. This work describes the molecular design of a p-type charge transport liquid crystalline polymer, in an attempt to control the factors responsible for both mobility and stability. Molecules were designed that were able to exhibit closely packed, π stacked morphologies, which can result in efficient intermolecular charge hopping and hence high mobility. Molecular manipulation of the conjugated π electron system was required to optimize the HOMO energy level, to both resist oxidation and be able to readily accept holes from a source electrode.

Introduction

The development of organic field effect transistors (OFETs) has generated a great deal of interest in the generation of solution processable organic semiconductors, which can combine both oxidative stability and high charge carrier mobility.[1−3] It has been shown that the charge carrier mobility is strongly dependent on the macroscopic organization of the molecules.[4−7] In particular, creation of organized macroscopic domains, in which there is molecular orientation of the π-conjugated molecular orbitals with respect to the substrate, and alignment on the macroscale with respect to the source and drain electrodes facilitate intermolecular charge transport. We have attempted to create this type of semiconductor macrostructure through the design of main chain liquid crystalline polymers, where supramolecular organization and alignment of the polymer chains can be enhanced through utilization of liquid crystalline mesophases occurring during the processing steps. Both lyotropic and thermotropic phases can induce highly ordered, closely packed structures, leading to high charge carrier mobilities within the domain boundaries.[8]

Poly(9,9-dialkyl)fluorenes[9,10] (PF) have been shown to be stable semiconductors. The charge carrier mobility of these polymers are however, limited by their steric inability to exhibit the two-dimensional lamellar π stacking morphology that has been shown, in the case of polyalkylthiophenes,[5] to be particularly effective in promoting intermolecular hopping, leading to high charge carrier mobilities. To address this limitation, a new class of semiconducting polymer, polyalkylidene fluorenes, have been synthesized, as shown in Figure 1. Polyalkylidene fluorenes have an sp^2-hybridized carbon at the 9-position, which permits the alkyl chains to adopt a coplanar conformation relative to the polymer backbone, thus facilitating cofacial aggregation. Cofacial, $\pi-\pi$ stacking morphology has been shown to lead to very small intermolecular distances (<4 Å) in the crystalline or liquid crystalline state.[11] In comparison, the carbon at the 9-position of poly(9,9-dialkylfluorene) is sp^3-hybridized, and therefore, the alkyl substituents at this position cannot extend in the plane of the fluorene unit, thus limiting the extent of π stacking.[12] The planar conformation of the polyalkylidenefluorene chain, stabilized by the intermolecular interactions, also enhances the effective conjugation along the length of the chain, which has been shown to reduce the ionization potential[13] and thus improve both charge injection, with respect to gold electrodes, as well as charge carrier mobility in a transistor device.

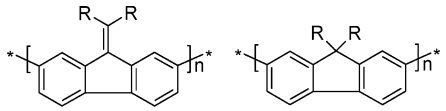

Figure 1. Chemical structure of polyalkylidene fluorene (a) and polyfluorene (b) (Where R = C_6H_{13} (P6AF), C_8H_{17} (P8AF), $C_{10}H_{21}$ (P10AF)).

Results and Discussion

Synthesis of Monomers. Alkylidene-substituted fluorenes containing methyl and ethyl side chains have previously been synthesized by the reaction of fluorenones with the appropriate secondary alkyl Grignard reagent, followed by dehydration of the resulting alcohol.[14] To provide polymers of good solubility, it was reasoned that the incorporation of longer alkyl chains was necessary. The drawbacks of the existing synthesis, namely the paucity of commercially available long chain secondary alkyl Grignards or their precursor halides and the tedious nature of their synthesis, necessitated the development of a new route to the starting monomers.

As outlined in Scheme 1, the monomers were conveniently synthesized in just two steps from commercially available 2,7-dibromofluorene. The initial step involved the formation of a ketene dithioacetal by condensation of a preformed fluorenyl anion with carbon disulfide, followed by an in situ alkylation of the resultant ketene

* Corresponding author. E-mail: iain.mcculloch@mercknbsc.co.uk.

10.1021/ma049798n CCC: $27.50
Published on Web 06/17/2004

Scheme 1. Synthetic Approach to Poly(alkylidene)fluorenes

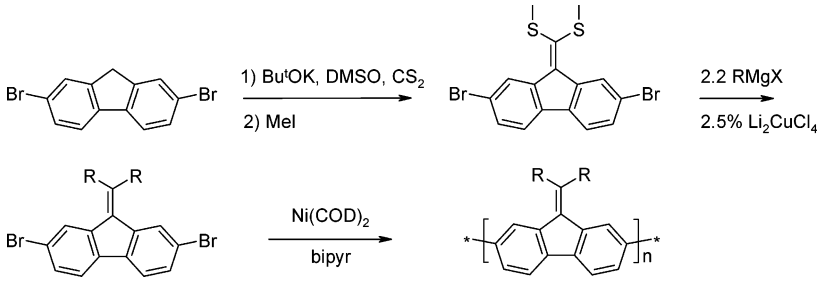

dithiolate anion with methyl iodide to give the dimethylated thioacetal in high yield. Treatment of the ketene dithioacetal with 2 equiv of an alkyl Grignard reagent in refluxing DME for 12 h initially resulted in moderate yields (20−25%) of the dialkylated product. This reaction presumably occurs via an addition−elimination sequence, with the intermediate carbanion at the bridgehead position stabilized by resonance. After some experimentation, it was found that the addition of a catalytic amount of Kuchi's salt (Li_2CuCl_4) both lowered the reaction temperatures and time and improved yields significantly. Derivatives containing hexyl to decyl side chains were synthesized in reasonable yields (50−60%). In contrast to unsubstituted dibenzofulvene, which readily reacts with itself or amine nucleophiles at room temperature,[15] the present compounds were stable under ambient conditions and in the presence of amine nucelophiles such as morpholine or piperidine.

An X-ray crystal structure for monomer C6AF reveals an essentially planar fluorene ring system, where the central alkylidene bond (C1−C14) lies in the plane of the fluorene ring system (Figure 2). There appears to be no steric strain between the C3, C12 hydrogen atoms of the fluorene ring and the vinylic hydrogen atoms (C15, C21), since there is no twist about the central double bond. Such a twist has been observed in bifluorenylidene derivatives.[16] The crystal packing indicates that the molecules pack in a staggered manner, with three different $\pi-\pi$ interactions apparent, ranging in distance from 3.73 to 3.82 Å. In contrast, the single crystal of 2,7-dibromo-9,9-dioctylfluorene exhibits no aromatic stacking because of the disposition of the alkyl chains.[12]

Synthesis and Characterization of Polymers. Polymerizations were performed under Yamamoto conditions.[17] The monomers were heated with a nickel(0) catalyst in a mixed DMF−toluene solvent for 48 h, followed by in situ end-capping the as-formed polymer with an excess of bromobenzene to remove any terminal bromine functionality. For both the hexyl- and octyl-substituted polymers, precipitation occurs during the course of the reaction, due to poor solubility of the growing polymer in the DMF/toluene solvent mixture. Purification was carried by out by precipitation of the reaction mixtures into methanol, followed by sequential Soxhlet extractions with methanol, acetone, and hexane to remove catalyst residues and low molecular weight oligomers. Finally, the polymers were dissolved in chloroform and then precipitated into methanol, affording yellow powders. Typical polymerization yields were low (~40%) for the short side chain (C6) polymers and improved to over 80% for side chain lengths of eight carbons and above. The low yield for the short chain polymer was attributed to the removal during workup of a high percentage of very low molecular weight oligomer that was formed due to low polymer solubility.

With the exception of C6PAF, all polymers exhibited good solubility in relatively nonpolar organic solvents, such as chloroform, tetrahydrofuran, and toluene. The structures of the polymers were characterized by spectroscopic methods. ^{1}H NMR spectra were obtained for the polymers at 50 °C in chloroform-*d*, since room-temperature measurements showed considerable broadening of the peaks. Figure 3 shows a representative polymer, C10PAF, in comparison with the respective monomer, C10AF. The signals for the three different aromatic protons in the fluorene unit are resolved as broad signals at δ 8.1, 7.8, and 7.6 ppm, with the alkylidene protons clearly visible at 2.9 ppm. The FT-IR spectra for pristine C10PAF is shown in Figure 4 and is consistent with the expected structure. Of note is the fact that no fluorenone resonance around 1720 cm^{-1} is observed.[18]

Molecular masses for the polymers were determined by GPC against polystyrene standards and are summarized in Table 1. These data should be taken with a degree of caution, since the values obtained for rigid-rod polymers are often an overestimation.[19,20] The hexyl- and octyl-substituted polymers both exhibited unimodal distributions with low molar masses. These low masses are probably a result of the polymer precipitating from the reaction mixture. For the more soluble decyl-substituted polymer, bimodal distributions were obtained with high polydispersities. The measurements were further complicated by the fact that the mass distributions for a given polymer were concentration and solvent dependent (Figure 5). Thus, in a THF solution of concentration 0.4 mg/mL, the main peak has an apparent molecular mass around 65 000 (15 min) with a smaller component centered around 15 000. However, on increasing the dilution 20-fold, the peak ratios change dramatically, with the smaller mass peak now dominating. The trend continues upon increasing dilution, but the high M_w peak is never completely absent. Solutions in chloroform, which is a better solvent for the polymer, exhibit a similar trend, although the high M_w peak is less prominent, even in the more concentrated solution. We attribute this behavior to a high propensity for the polymer to aggregate in solution, especially in a Θ solvent such as THF. This is further demonstrated by the fact that the UV/vis spectra of the thin film is almost identical to the solution spectra in THF.

Optical Properties. Alkylidene fluorene polymers have a bathochromic (red) optical absorption maximum in comparison to polyfluorenes, as illustrated in Figure 6. This reduced band gap is primarily due to the enhanced planarization of the conjugated polymer backbone, which is particularly pronounced in the solid state spectra. In addition, a shoulder can be clearly seen at about 420 nm, which is believed to be due to effects associated with aggregation.[11,21] Upon heating this

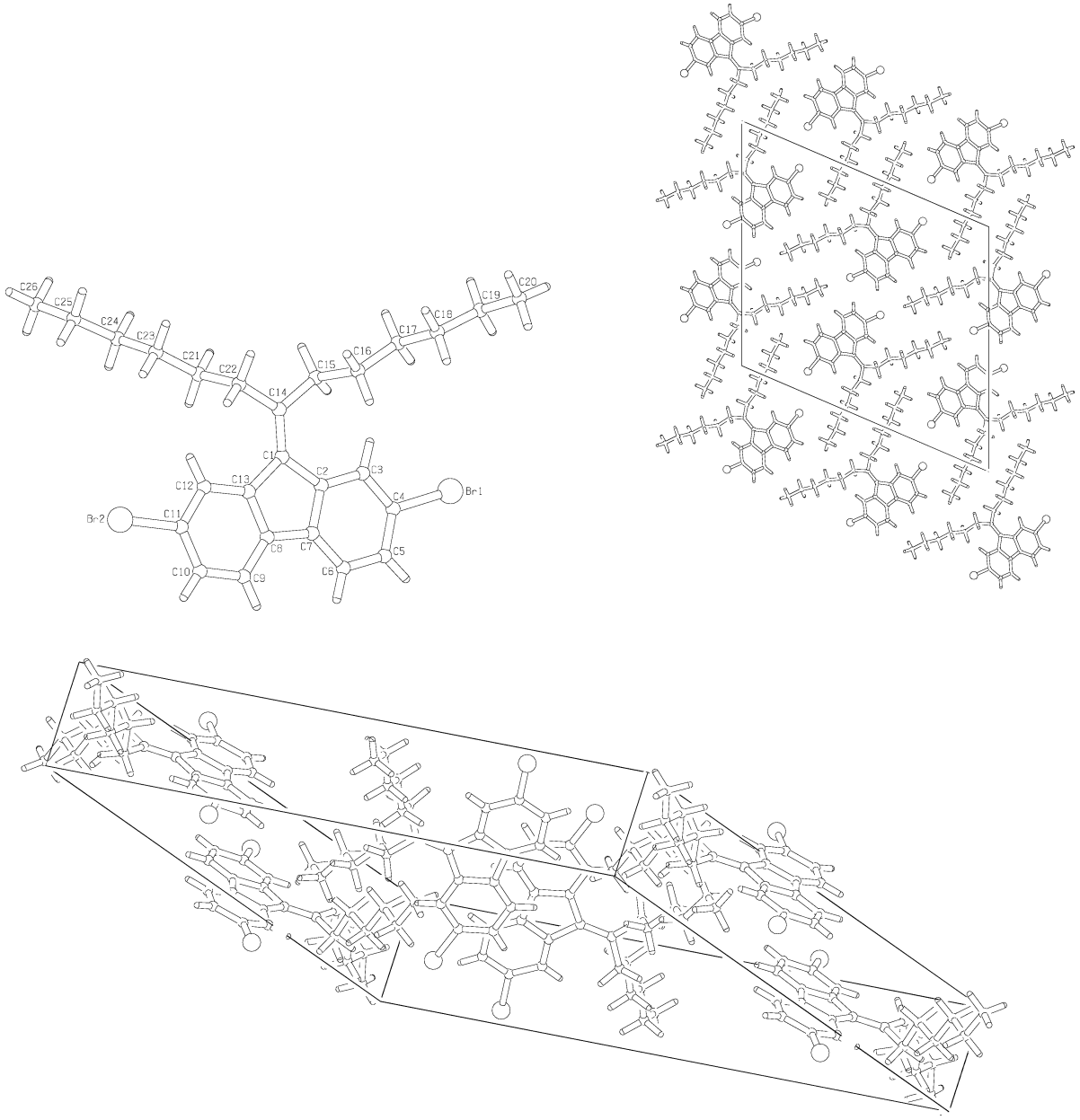

Figure 2. ORTEP single crystal and crystal packing of C6AF monomer.

shoulder collapses, as shown in Figure 7. The electronic orbital band structure, as determined by ultraviolet photoelectron spectroscopy and reported elsewhere,[13] confirms that the ionization potential of alkylidene fluorene polymers has been reduced by about 0.4 eV, to 5.5 eV, as compared to polyfluorene,[22] which is high enough to be stable to oxidation in air.[23]

The thermal behavior of polyalkylidene fluorenes was complicated to interpret, due to small entropy differences on phase changes and overlapping processes. In general, complimentary techniques of differential scanning calorimetry (DSC) and optical microscopy were required to identify phases. All polymers exhibited a nematic mesophase, which can be identified by the characteristic Schlieren texture observed by polarized optical microscopy, as shown in Figure 8. The effect of increasing side chain length on the thermal behavior of the polymers was not shown to be very significant. Although it would be expected that longer side chains, acting like "bound solvent", would lower the melt point of the polymer main chains, this was not conclusively shown. One explanation of this is that the molecular weight of the short chain polymers (C6 and C8) is not high enough to have reached their maximum thermal properties and hence any trend would be suppressed. All polymers exhibited a glass transition at about 140 °C, believed to be too high to be related to side chain melting. The sensitivity of the DSC instrument was not sufficient to identify this transition. Broad melt points were observed within the temperature range from 240 to 260 °C. Clearing points for all polymers were only observed by microscopy. The clearing points appear to be close to the onset of degradation, and some signs of degradation at temperatures above the clearing point are evident by microscopy as darkening around the edges of the slide. On slow cooling through the mesophase, crystallization was observed by polarized microscopy. Rapid cooling from the mesophase quenches in a thermodynamically unstable "glassy nematic phase", which on heating exhibits a more pronounced glass transition. No evidence of smectic phases could be observed by optical microscopy, although this may be

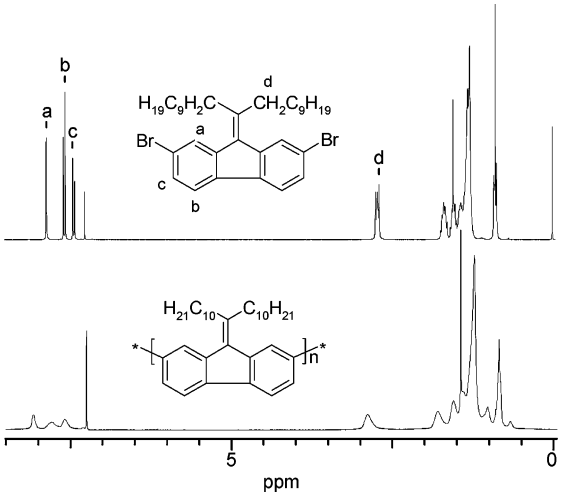

Figure 3. ^{1}H NMR spectra of polymer C10PAF at 50 °C in comparison to monomer C10AF.

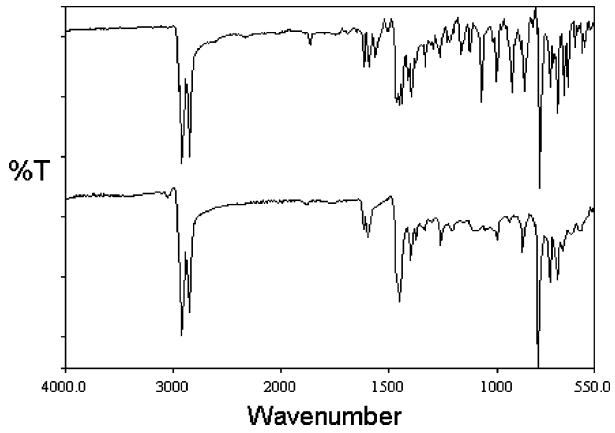

Figure 4. FTIR of C10AF (top) and C10PAF (bottom).

Table 1. Polymer Molecular Weight Data

polymer	M_n[a]	D[a]
C6PAF	4000	1.2
C8PAF	5400	1.2
C10PAF	14000	2.5

[a] Determined by GPC in $CHCl_3$ against polystyrene standards.

due to the nature of the annealing processes and heat rates used. A summary of the thermal properties of this polymer series is shown in Table 2.

Transistor Fabrication and Measurement. Thin-film organic field-effect transistors (OFETs) were fabricated on highly doped silicon substrates with a 230 nm thick thermally grown silicon oxide (SiO_2) insulating layer, where the substrate served as a common gate electrode. Transistor source-drain gold electrodes were photolithographically defined on the SiO_2 layer. Prior to organic semiconductor deposition, FET substrates were treated with a silylating agent hexamethyldisilazane (HMDS). Thin semiconductor films were then deposited by spin-coating polymer solutions in chloroform (0.4−1 wt %) on FET substrates. The electrical characterization of the transistor devices was carried out in a dry nitrogen atmosphere using a computer-controlled Agilent 4155C semiconductor parameter analyzer.

Electrical Properties. Transistor characteristics of C6PAF, C8PAF, and C10PAF were measured on as-spun films. Thermal treatment followed, when samples were heated to the nematic phase in N_2 atmosphere, held at this temperature, and then cooled to room temperature. Under negative gate bias, devices showed typical p-type behavior with good current modulation (on/off ratio of 10^4−10^6) and well-defined linear and saturation regimes, as shown in Figure 9 for C10PAF. Field effect mobility was calculated in the saturation regime [$V_d > (V_g - V_0)$] using eq 1

$$\left(\frac{dI_d^{sat}}{dV_e}\right)_{V_d} = \frac{WC_i}{L}\mu^{sat}(V_g - V_0) \qquad (1)$$

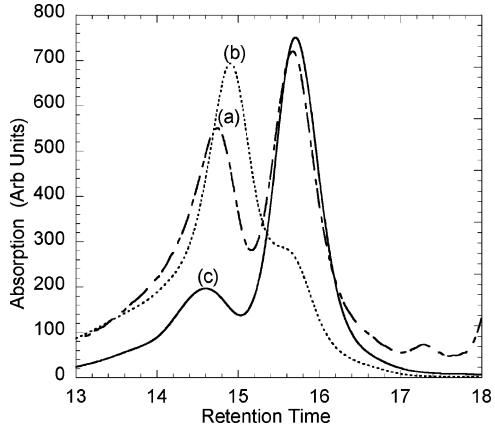

Figure 5. GPC traces for (a) 0.002 mg/mL solution in THF, (b) 0.4 mg/mL solution in THF, (c) 0.4 mg/mL solution in chloroform

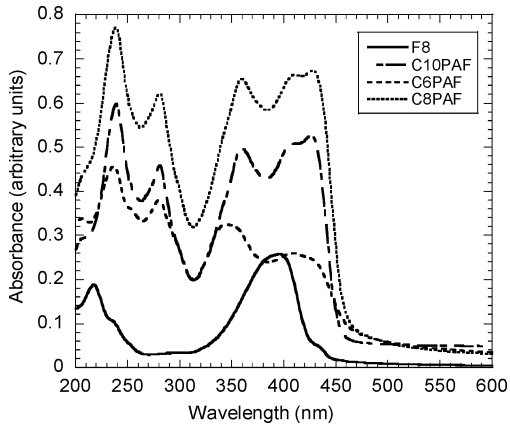

Figure 6. Optical absorption as spin cast films. F8 is poly-(9,9-dioctylfluorene).

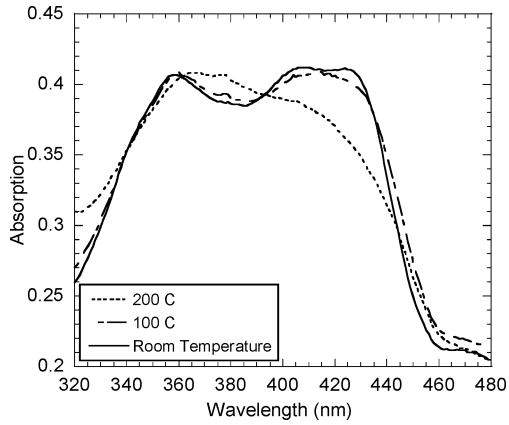

Figure 7. Change in absorption upon heating a thin film of C10PAF.

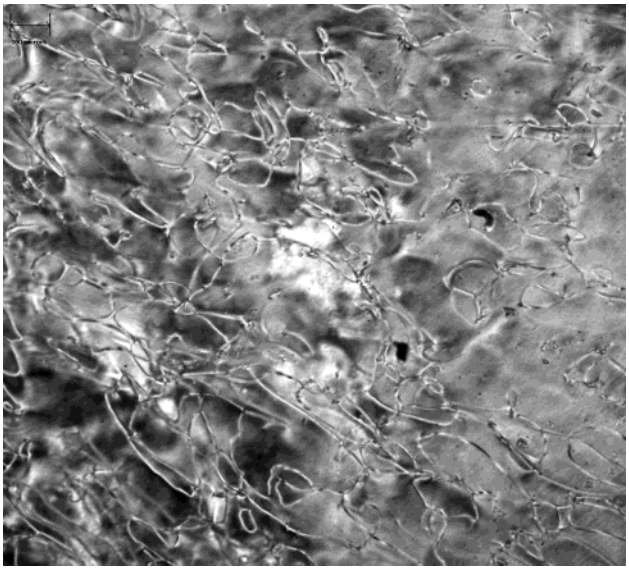

Figure 8. Micrograph under crossed polarizers illustrating the threaded texture of C10PAF in nematic phase.

Table 2. Thermal Behavior for Polymers

polymer	T_g (°C)	T_m (°C)	T_{cl} (°C)
C6PAF	140	235−245	390
C8PAF	150	230−240	375
C10PAF	140	230−240	380

where W is the channel width, L the channel length, C_i the capacitance of the insulating layer, V_g the gate voltage, and V_0 the turn-on voltage. Turn-on voltage (V_0) was determined as the onset of source-drain current (Figure 9a).

Field-effect mobilities for C6PAF, C8PAF, and C10PAF are summarized in Table 3. In as-spun films, all polymers showed a field-effect mobility from 1×10^{-4} to 9×10^{-4} cm^2/V s resulting from unoptimized film morphology. The degree of order for the polymers improved after thermal treatment where samples were annealed in the nematic phase, and as a result, increased field effect mobilities from 4×10^{-4} to 2×10^{-3} cm^2/Vs were observed. Maximum current observed in annealed C10PAF FETs with channel length $L = 10\ \mu$m and channel width $W = 2$ cm reached 0.1 mA and on/off ratio exceeded 10^6.

It has been observed that the optimum annealing temperature was in the range 170−190 °C with a total annealing time of about 30 min. At lower annealing temperatures, polymer mobilities did not reach maximum values, whereas higher temperatures resulted in reduced charge transport.

Turn-on voltages for all polymer FET samples were quite high (between −5 and −24 V) with some variations from batch to batch. Such high turn-on voltages can be explained by an approximately 0.4 eV mismatch between the work function of gold electrodes (∼5.1 eV)[24] and the polymer HOMO level (∼5.5 eV). This also resulted in detectable contact resistance, as evidenced by a slight curvature of source-drain currents in output characteristics (Figure 9b) at low source-drain voltages (0 to −3V).

Summary

A new methodology for the synthesis of symmetrically substituted alkylidene fluorenes was demonstrated. The resultant monomers were successfully polymerized under Yamamoto conditions, to form a novel class of soluble, conjugated main chain semiconducting polymers. A series of homologues, differing in the length of alkyl side chains, were prepared, all of which were found to both strongly aggregate in solution and exhibit nematic thermotropic mesophases. Field effect transistors were fabricated, utilizing these polymers as the semiconducting layer, and on annealing above the glass transition, field-effect mobilities of up to 2×10^{-3} cm^2/V s were reached. These good charge transport properties, together with high current modulation (on/off ratio up to 10^6), make this material an attractive candidate for organic electronic applications.

Experimental Section

General. ^{1}H and ^{13}C NMR spectra were recorded on a Bruker AV-300 (300 MHz), using the residual solvent resonance of $CDCl_3$ or TMS as an internal reference, and are given in ppm. IR spectra were obtained on a Perkin-Elmer Spectrum One FTIR. UV/vis spectra were obtained on a Perkin-Elmer Lamda 9 spectrometer. Microanalyses were obtained with an Elementar Vario EL analyzer. Mass spectra were obtained either from an Agilent GC−MS using a 6890 series GC with a 5973 MSD (EI) or a Bruker Esquire 3000+ (ESI). Molecular weight determinations were carried out in chloroform solution on an Agilent 1100 series HPLC using two Polymer Laboratories mixed B columns in series, and the system was calibrated against narrow weight PL polystyrene calibration standards. DSC measurements were performed on a Perkin-Elmer DSC 7 under nitrogen. All starting materials and reagents were purchased from Aldrich Chemicals or Lancaster Chemicals and used as received, with the exception of 1,5-bis-(cyclooctadiene)nickel(0) (Strem Chemicals). Anhydrous solvents were purchased from Romil Ltd and transferred using standard Schlenk line techniques. Column chromatography and TLC were performed on silica gel 60 (70−230 mesh, Merck) and silica gel F_{254} plates (Merck), respectively. Petrol refers to the fraction boiling at 40−60 °C.

2,7-Dibromo-9-(bis(methylsulfanyl)methylene)fluorene. Sodium *tert*-butoxide (31.14 g, 0.324 mol) was added in portions to a mechanically stirred solution of 2,7-dibromofluorene (50.00 g, 0.154 mol) in anhydrous DMSO (1 L) at room temperature under nitrogen. Carbon disulfide (12.94 g, 0.170 mol) was added via syringe and the reaction mixture was stirred for 10 min. Methyl iodide (46.00 g, 0.324 mol) was added via a dropping funnel over 5 min and the reaction mixture was stirred for 4 h. The reaction mixture was poured into ice−water (1 L), and concentrated ammonia (50 mL) was added to quench any remaining methyl iodide. The resulting precipitate was filtered, washed with water, dried, and recrystallized from ethyl acetate:THF (2:1) to afford the product as bright yellow needles (55.15 g, 83%). Mp: 155−156.5 °C. ^{1}H NMR ($CDCl_3$, 300 MHz): δ (ppm) 8.90 (s, 2H), 7.51 (d, ^3J = 8.2 Hz, 2H), 7.42 (d, ^3J = 8.2 Hz, 2H), 2.57 (s, 6H). ^{13}C NMR ($CDCl_3$, 75 MHz): δ (ppm) 147.30, 139.40, 137.54, 134.28, 130.33, 129.13, 121.21, 120.41, 19.14. IR 3097 (w), 2921 (w), 1882 (w), 1560 (m), 1517 (s), 1440 (s), 1390 (s), 1065 (m), 943 (m). Anal. Calcd for $C_{16}H_{12}Br_2S_2$: C, 44.9; H, 2.8. Found: C, 44.7; H, 3.1. MS (EI): m/z 430 (M^+, 50), 428 (M^+, 100), 426 (M^+, 50).

The general procedure for the synthesis of the alkylidene monomers is exemplified by the following synthesis:

2,7-Dibromo-9-(1′-decylundecylidene)fluorene. To a stirred solution of 2,7-dibromo-9-(bis(methylsulfanyl)methylene)fluorene (10.00 g, 23.35 mmol) in anhydrous THF (150 mL) at −5 °C under nitrogen was added lithium tetrachlorocuprate (6 mL of a 0.1 M solution in THF, 0.6 mmol), followed by the addition of decylmagnesium bromide (52 mL of a 1.0 M solution in diethyl ether, 52 mmol) over 30 min, keeping the temperature below 0 °C throughout. The reaction was stirred for a further 4 h at −5 °C and then quenched by the addition of 10% sodium hydroxide (100 mL). The reaction was stirred for 10 min and then filtered through Celite, washing through

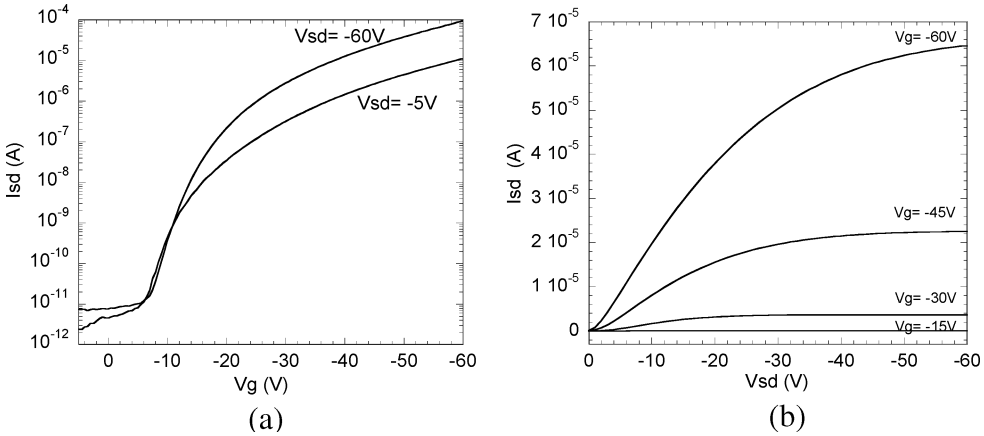

Figure 9. Transfer (a) and output (b) characteristics of a C10PAF transistor with channel length $L = 10\ \mu$m and channel width $W = 2$ cm.

Table 3. Electronic Properties for Polymers

	μ_{sat} (cm^2/V s)		
polymer	as-spun	annealed	on/off
C6PAF	1×10^{-4}	4×10^{-4}	10^4
C8PAF	3×10^{-4}	1×10^{-3}	10^4
C10PAF	9×10^{-4}	2×10^{-3}	10^6

with ethyl acetate. The resulting layers were separated, and the aqueous layer further extracted with ethyl acetate. The combined organic extracts were washed 10% aqueous solution of sodium hydroxide (100 mL), saturated sodium metabisulfite (100 mL), and brine (100 mL), and then dried over sodium sulfate and concentrated in vacuo. The residue was filtered through a layer of silica ($5 \times 5 \times 10$ cm^2) with a layer of basic alumina ($5 \times 5 \times 1$ cm^2) on top and washed through with petrol (1.5 L). The filtrate was concentrated in vacuo. Recrystallization from isohexane at −38 °C yielded the product as pale yellow needles (7.47 g, 52%). Mp: 35.5−36.5 °C. ^{1}H NMR ($CDCl_3$, 300 MHz): δ (ppm) 7.85 (d, $^3J = 1.5$ Hz 2H,), 7.56 (d, $^3J = 8.1$ Hz, 2H), 7.42 (dd, $^3J = 8.1$ & 1.5 Hz, 2H), 2.71 (t, $^3J = 8.3$ Hz, 4H), 1.68 (m, 4H), 1.53 (m, 4H), 1.42 (m, $4H_2$), 1.28 (m, 20H), 0.89 (t, $^3J = 6.7$ Hz, 6H). ^{13}C NMR ($CDCl_3$, 75 MHz): δ (ppm) 155.27, 139.93, 137.40, 129.79, 129.34, 127.90, 121.13, 120.46, 37.52, 31.93, 30.06, 29.64, 29.60, 29.43, 29.34, 27.80, 22.71, 14.14. IR (thin film): 2952 (m), 2919 (s), 2849 (m), 1866 (w), 1617 (m), 1595 (m), 1465 (m), 1439 (m), 1072 (m), 932 (m), 816 (s) cm^{-1}. Anal. Calcd for $C_{34}H_{48}Br_2$: C, 66.2; H, 7.85. Found: C, 66.1; H, 7.3. MS (EI): *m*/*z* 618 (M^+, 5), 616 (M^+, 10), 614 (M^+, 5), 476 ($M^+ - C_{10}H_{21}$, 10), 336 ($M^+ - C_{20}H_{42}$, 100).

2,7-Dibromo-9-(1′-hexylheptylidene)fluorene was synthesized from 2,7-dibromo-9-(bis(methylsulfanyl)methylene)-fluorene (5.20 g, 12 mmol) and hexylmagnesium bromide (15 mL of a 2 M solution in diethyl ether, 30 mmol) following the procedure described above. Prior to final chromatographic purification, dodecane ($C_{12}H_{26}$) byproduct was removed by Kugelrohr distillation. Recrystallization from isohexane yielded the product as pale yellow needles (3.20 g, 53%): mp 31−32 °C. ^{1}H NMR ($CDCl_3$, 300 MHz): δ (ppm) 7.84 (d, $^3J = 1.5$ Hz, 2H), 7.55 (d, $^3J = 8.1$ Hz, 2H), 7.41 (dd, $^3J = 8.1$ & 1.5 Hz, 2H), 2.70 (t, $^3J = 8.3$ Hz, 4H), 1.67 (m, 4H), 1.55 (m, 4H), 1.39 (m, 8H), 0.94 (t, $^3J = 6.9$ Hz, 6H). ^{13}C NMR ($CDCl_3$, 75 MHz): δ (ppm) 155.24, 139.96, 137.43, 129.82, 129.37, 127.91, 121.16, 120.49, 37.55, 31.66, 29.74, 27.79, 22.69, 14.13. IR (thin film): 2958 (m), 2921 (s), 2854 (s), 1877 (w), 1617 (m), 1595 (m), 1561 (m), 1456 (m), 1398 (m), 1074 (m), 937 (s) cm^{-1}. Anal. Calcd for $C_{26}H_{32}Br_2$: C, 61.9; H, 6.4. Found: C, 61.8; H, 6.1. MS (EI): *m*/*z* 506 (M^+, 10), 504 (M^+, 20), 502 (M^+, 10), 420 ($M^+ - C_6H_{13}$, 18), 336 ($M^+ - C_{12}H_{26}$, 100).

2,7-Dibromo-9-(1′-octylnonylidene)fluorene was synthesized by reaction of 2,7-dibromo-9-(bis(methylsulfanyl)-methylene)fluorene (5.20 g, 12 mmol) with octylmagnesium bromide (13 mL of a 2 M solution in diethyl ether, 26 mmol) following the procedure described above. Purification by column chromatography (eluent: petroleum ether 40−60) and recrystallization from isohexane yielded the product as pale yellow needles (3.60 g, 54%). Mp: 34−35 °C. ^{1}H NMR ($CDCl_3$, 300 MHz): δ (ppm) 7.86 (s, $^3J = 1.4$ Hz 2H), 7.58 (d, $^3J = 8.1$ Hz, 2H), 7.43 (dd, $^3J = 8.1$ & 1.4 Hz, 2H), 2.72 (t, $^3J = 8.3$ Hz, 4H), 1.68 (m, 4H), 1.54 (m, 4H), 1.32 (m, 8H), 0.90 (t, $^3J = 6.7$ Hz, 6H). ^{13}C NMR ($CDCl_3$, 75 MHz): δ (ppm) 155.31, 139.95, 137.42, 129.80, 129.37, 127.92, 121.15, 120.49, 37.54, 31.85, 30.06, 29.40, 29.30, 27.82, 22.68, 14.14. IR (thin film): 2954 (m), 2922 (s), 2853 (m), 1876 (w), 1611 (m), 1593 (m), 1439 (m), 1072 (m), 938 (m), 816 (vs) cm^{-1}. Anal. Calcd for $C_{30}H_{40}Br_2$: C, 64.3; H, 7.2. Found: C, 64.6; H, 6.7. MS (EI): *m*/*z* 562 (M^+, 10), 560 (M^+, 20), 558 (M^+, 10).

The general procedure for the synthesis of the alkylidene polymers is exemplified below:

Poly[9-(1′-decylundecylidene)fluorene-2,7′-diyl] (C10PAF). A Schlenk tube was charged with bis(1,5-cyclooctadiene)nickel(0) (2.000 g, 7.271 mmol) and 2,2′-bipyridyl (0.973 g, 6.233 mmol) under nitrogen. 1,5-Cyclooctadiene (0.64 mL, 5.218 mmol) and anhydrous *N*,*N*-dimethylformamide (20 mL) were added, and the reaction mixture was stirred at 60 °C for 30 min. A solution of 2,7-dibromo-9-(1′-decylundecylidene)fluorene (3.202 g, 5.194 mmol) in anhydrous toluene (40 mL) was added and the reaction mixture was stirred at 80 °C for 24 h with the exclusion of light. The reaction mixture was cooled to room temperature and added to acidic methanol (400 mL). The suspension was stirred for 1 h. The polymer was filtered off, washed with water and then methanol, and dried under vacuum. The polymer was washed (via Soxhlet extraction) with methanol for 24 h, acetone for 24 h, and isohexane for 24 h. The polymer was dried under vacuum and dissolved in hot chloroform (100 mL). The hot chloroform solution was filtered through a sintered funnel and concentrated in vacuo to a minimum volume. The concentrated chloroform solution was precipitated from methanol (500 mL). The polymer was filtered off and dried under vacuum to yield the polymer as a yellow solid (2.02 g, 85%). ^{1}H NMR ($CDCl_3$, 50 °C, 300 MHz): δ 8.08 (br, 2H), 7.79 (br, 2H), 7.60 (br, 2H), 2.89 (br, 4H), 1.80 (br, 4H), 1.7−0.7 (m, 36H). Anal. Calcd for $C_{34}H_{50}$: C, 89.0; H, 11.0. Found: C, 89.0; H, 11.4; Br, <0.3. IR (thin film): 2920 (s), 2850 (s), 1620 (m), 1597 (m), 1455 (s), 1400 (m), 883 (m), 811 (vs). λ_{max} ($CHCl_3$): 409, 360, 344, 280 (film) 428, 406 (sh), 358, 280, 240 nm. GPC ($CHCl_3$): M_n 14 000 g/mol, $D = 2.5$.

Poly[9-(1′-hexylheptylidene)fluorene-2,7′-diyl] (C6PAF). Polymerization of 2,7-dibromo-9-(1′-hexylheptylidene)fluorene (0.500 g, 0.991 mmol) by the method described above afforded the product as a yellow solid (0.130 g, 38%). ^{1}H NMR ($CDCl_3$, 50 °C, 300 MHz): δ 8.10 (br. 2H), 7.88 (br d, 2H), 7.63 (br d, 2H), 2.93 (br, 4H), 1.84 (br, 4H), 1.7−1.2 (m, 12H), 0.9 (br t, 6H). IR (thin film): 2921 (s), 2853 (s), 1620 (m), 1597 (m), 1454 (s), 1400 (m), 881 (m), 809 (vs). Anal. Calcd for $C_{26}H_{34}$: C, 90.1; H, 9.9. Found: C, 90.0; H, 8.9. λ_{max} ($CHCl_3$): 399, 355, 340

(sh), 278 (film) 407, 342, 280, 235 nm. GPC ($CHCl_3$): M_n 4000 g/mol, $D = 1.2$.

Poly[9-(1′-octylnonylidene)fluorene-2,7′-diyl] (C8PAF). Polymerization of 2,7-dibromo-9-(1′-octylnonylidene)fluorene (1.00 g, 1.78 mmol) by the method described above afforded the product as a yellow solid (0.600 g, 83%). ^{1}H NMR ($CDCl_3$, 50 °C, 300 MHz): δ 8.09 (br, 2H), 7.86 (br, 2H), 7.62 (br, 2H), 2.92 (br, 4H), 1.83 (br, 4H), 1.7−0.7 (m, 28H). Anal. Calcd for $C_{30}H_{42}$: C, 89.5; H, 10.5. Found: C, 89.4; H, 11.4. IR (thin film): 2920 (s), 2850 (s), 1617 (m), 1598 (w), 1455 (s), 1400 (m), 883 (m), 811 (vs). λ_{max} ($CHCl_3$): 409, 360, 340 (sh), 280, (film) 429, 409 (sh), 358, 280, 238 nm. GPC ($CHCl_3$): M_n 5400 g/mol, $D = 1.2$.

Acknowledgment. The authors would like to thank Dr. Simon Coles and Prof. Mike Hursthouse of the University of Southampton for obtaining the X-ray crystallography data.

Supporting Information Available: Table of X-ray crystallographic data for structural determination (CIF). This material is available free of charge via the Internet at http://pubs.acs.org.

References and Notes

(1) Dimitrakopoulos, C. D.; Malenfant, P. R. L. *Adv. Mater.* **2002**, *14*, 99−117.
(2) Katz, H. E.; Bao, Z.; Gilat, S. L. *Acc. Chem. Res.* **2001**, *34*, 359−369.
(3) Horowitz, G. *Adv. Mater.* **1998**, *10*, 365−377.
(4) Garnier, F. *Acc. Chem. Res.* **1999**, *32*, 209−215.
(5) Sirringhaus, H.; Brown, P. J.; Friend, R. H.; Nielsen, M. M.; Bechgaard, K.; Langeveld-Voss, B. M. W.; Spiering, A. J. H.; Janssen, R. A. J.; Meijer, E. W.; Herwig, P.; de Leeuw, D. M. *Nature* **1999**, *401*, 685−688.
(6) Sirringhaus, H.; Brown, P. J.; Friend, R. H.; Nielsen, M. M.; Bechgaard, K.; Langeveld-Voss, B. M. W.; Spiering, A. J. H.; Janssen, R. A. J.; Meijer, E. W. *Synth. Met.* **2000**, *111−112*, 129−132.
(7) Chen, X. L.; Lovinger, A. J.; Bao, Z.; Sapjeta, J. *Chem. Mater.* **2001**, *13*, 1341−1348.
(8) Sirringhaus, H.; Wilson, R. J.; Friend, R. H.; Inbasekaran, M.; Wu, W.; Woo, E. P.; Grell, M.; Bradley, D. D. C. *Appl. Phys. Lett.* **2000**, *77*, 406−408.
(9) Scherf, U.; List, E. J. W. *Adv. Mater.* **2002**, *14*, 477−487.
(10) Leclerc, M. *Polymer* **2001**, *39*, 2867−2873.
(11) Yamamoto, T.; Komarudin, D.; Arai, M.; Lee, B.-L.; Suganuma, H.; Asakawa, N.; Inoue, Y.; Kubota, K.; Sasaki, S.; Fukuda, T.; Matsuda, H. *J. Am. Chem. Soc.* **1998**, *120*, 2047−2058.
(12) Leclerc, M.; Ranger, M.; Belanger-Gariepy, F. *Acta Crystallogr. C* **1998**, *54*, 799−801.
(13) Osikowicz, W.; Murdey, R.; Giles, M.; Heeney, M.; Tierney, S.; McCulloch, I.; Salaneck, W. R. *Chem. Phys. Lett.* **2004**, *385*, 184−188.
(14) Ranger, M.; Leclerc, M. *Macromolecules* **1999**, *32*, 3306−3313.
(15) Carpino, L. A.; Han, G. Y. *J. Am. Chem. Soc.* **1970**, *92*, 5748−5749.
(16) Bailey, N. A.; Hull, S. E. *Acta Crystallogr. B* **1978**, *34*, 3289−3295.
(17) Yamamoto, T.; Morita, A.; Miyazaki, Y.; Maruyama, T.; Wakayama, H.; Zhou, Z.; Nakamura, Y.; Kanbara, T.; Sasaki, S.; Kubota, K. *Macromolecules* **1992**, *25*, 1214−1223.
(18) List, E. J. W.; Guentner, R.; de Freitas, P. S.; Scherf, U. *Adv. Mater.* **2002**, *14*, 374−378.
(19) Grell, M.; Bradley, D. D. C.; Long, X.; Chamberlain, T.; Inbasekaran, M.; Woo, E. P.; Soliman, M. *Acta Polym.* **1998**, *49*, 439−444.
(20) Demadrille, R.; Rannou, P.; Bleuse, J.; Oddou, J.-L.; Pron, A.; Zagorska, M. *Macromolecules* **2003**, *36*, 7045−7054.
(21) Koren, A. B.; Curtis, M. D.; Kampf, J. W. *Chem. Mater.* **2000**, *12*, 1519−1522.
(22) Janietz, S.; Bradley, D. D. C.; Grell, M.; Giebeler, C.; Inbasekaran, M.; Woo, E. P. *Appl. Phys. Lett.* **1998**, *73*, 2453−2455.
(23) de Leeuw, D. M.; Simenon, M. M. J.; Brown, A. R.; Einerhand, R. E. F. *Synthetic Metals* **1997**, *87*, 53−59.
(24) Meijer, E. J.; de Leeuw, D. M.; Setayesh, S.; Van Veenendaaal, E.; Huisman, B.-H.; Blom, P. W. M.; Hummelen, J. C.; Scherf, U.; Klapwijk, T. M. *Nat. Mater.* **2003**, *2*, 678−682.

MA049798N